THE JOURNAL OF BIOLOGICAL CHEMISTRY VOL. 283, NO. 28, pp. 19626–19635, July 11, 2008

Specificity of the Chromodomain Y Chromosome Family of Chromodomains for Lysine-methylated ARK(S/T) Motifs*[S]

Received for publication, April 4, 2008, and in revised form, April 29, 2008 Published, JBC Papers in Press, May 1, 2008, DOI 10.1074/jbc.M802655200

Wolfgang Fischle[‡§¶1,2], **Henriette Franz**[¶1], **Steven A. Jacobs**[‡3], **C. David Allis**[‡§], **and Sepideh Khorasanizadeh**[‡4]

From the [‡]*Department of Biochemistry and Molecular Genetics, University of Virginia Health System, Charlottesville, Virginia 22908-0733,* [§]*Laboratory of Chromatin Biology, The Rockefeller University, New York, New York 10021, and* [¶]*Laboratory of Chromatin Biochemistry, Max Planck Institute for Biophysical Chemistry, 37077 Göttingen, Germany*

Previous studies have shown two homologous chromodomain modules in the HP1 and Polycomb proteins exhibit discriminatory binding to related methyllysine residues (embedded in ARKS motifs) of the histone H3 tail. Methylated ARK(S/T) motifs have recently been identified in other chromatin factors (*e.g.* linker histone H1.4 and lysine methyltransferase G9a). These are thought to function as peripheral docking sites for the HP1 chromodomain. In vertebrates, HP1-like chromodomains are also present in the chromodomain Y chromosome (CDY) family of proteins adjacent to a putative catalytic motif. The human genome encodes three CDY family proteins, CDY, CDYL, and CDYL2. These have putative functions ranging from establishment of histone H4 acetylation during spermiogenesis to regulation of transcription co-repressor complexes. To delineate the biochemical functions of the CDY family chromodomains, we analyzed their specificity of methyllysine recognition. We detected substantial differences among these factors. The CDY chromodomain exhibits discriminatory binding to lysine-methylated ARK(S/T) motifs, whereas the CDYL2 chromodomain binds with comparable strength to multiple ARK(S/T) motifs. Interestingly, subtle amino acid changes in the CDYL chromodomain prohibit such binding interactions *in vitro* and *in vivo*. However, point mutations can rescue binding. In support of the *in vitro* binding properties of the chromodomains, the full-length CDY family proteins exhibit substantial variability in chromatin localization. Our studies underscore the significance of subtle sequence differences in a conserved signaling module for diverse epigenetic regulatory pathways.

The human Y chromosome has been thoroughly sequenced and compared with partially sequenced Y chromosomes of chimpanzee and mouse (1–3). The Y chromosomes are believed to be enriched in genes essential for spermatogenesis and testis development. Interstitial Y chromosome deletions are associated with spermatogenic failure and male infertility (1, 4, 5). One gene that is present in multiple copies on the human Y chromosome is CDY,[5] which exhibits testis-specific expression (1). Interestingly, the mouse Y chromosome does not encode CDY, suggesting a developmentally advanced usage of CDY in primates (3).

The human CDY gene seems to be derived from the autosomal homologs CDYL or CDYL2 (Fig. 1, *A* and *B*) (6). CDYL is ubiquitously expressed, whereas CDYL2 exhibits selective expression in tissues of testis, prostate, spleen, and leukocytes (6). The mouse genome also encodes related CDYL and CDYL2 genes (Fig. 1*B*). The presence of CDY-like genes appears to be a hallmark of echinoderm and vertebrate genomes. In sea urchin and chicken genomes we found only one CDY-like gene that corresponds to mammalian CDYL2 (Fig. 1*B*).

CDY family proteins have two conserved domains implicated in histone modification and recognition; that is, a chromodomain followed by an enoyl-coenzyme A hydratase/isomerase (*ECH*) putative catalytic domain (Fig. 1*A*). Previously, it was shown that the chromodomain of human CDY interacts with methylated lysine 9 of the histone H3 tail (H3K9me) (7). The ECH domain has been implicated in conflicting chromatin modification processes. One function of this domain is acetylation of germ line histone H4 (8). Another function is direct recruitment of histone deacetylases to sites within somatic cells (9).

Epigenetic control of gene expression hinges on effecter recognition modules that help establish appropriate methyllysine-dependent interactions with chromatin (for review, see Ref. 10). The HP1 and Polycomb chromodomains (Fig. 1*B*), which are similar to the chromodomains of CDY family proteins, distinguish two methylated lysine residues within ARKS motifs in the H3 tail (H3K9me and H3K27me) (11–16). Sequences immediately preceding the ARK(S/T) motif impact on the specificity of chromodomain interactions. HP1 chromodomains are subject to a binary methyl-phos switch as they are prohibited from interaction with H3K9me3 upon phosphorylation of the adjacent serine 10 in the H3 tail (H3S10ph) (17–20).

Additional complexity in epigenetic control arises from usage of histone variants. For example, substitutions of histone H3 with variants results in indexing of chromatin for transcriptional activation or repression (22, 23), and an H3 barcode

* This work was supported, in whole or in part, by National Institutes of Health Grants GM064786 (to S. K.), GM63959, and GM53512 (to C. D. A.). This work was also supported by the Max Planck Society (to W. F.). The costs of publication of this article were defrayed in part by the payment of page charges. This article must therefore be hereby marked "*advertisement*" in accordance with 18 U.S.C. Section 1734 solely to indicate this fact.

[S] The on-line version of this article (available at http://www.jbc.org) contains supplemental Figs. S1–S3.

[1] These authors contributed equally to this work.
[2] A Robert Black fellow of the Damon Runyon Cancer Research Foundation. To whom correspondence may be addressed. E-mail: wfischl@gwdg.de.
[3] Present address: Centocor Research & Development, Radnor, PA, 19087.
[4] To whom correspondence may be addressed. E-mail: khorasan@virginia.edu.

[5] The abbreviations used are: CDY, chromodomain Y chromosome; ECH, enoyl-coenzyme A hydratase/isomerase; PBS, phosphate-buffered saline; DAPI, 4′,6-diamidino-2-phenylindole; MBP, maltose-binding protein.

hypothesis has been proposed (24). In human testis, three somatic histone H3 variants (H3.1, H3.2, and H3.3) are encoded together with a testis-specific subtype (H3t) (25). These variants have no amino acid changes N-terminal to the ARKS motifs, except in the H3t subtype. Although mass spectrometry has identified *in vivo* methylation of H3tK27 (26), an effector binding module has not yet been reported. Another lysine-methylated ARKS motif is found in the N-terminal tail of a linker histone H1 subtype in humans (H1.4K26) (27, 28).

An ARKT mimic of H3K9me has also been identified in the lysine methyltransferase G9a (G9aKme), suggesting a broader usage of ARK(S/T) motifs in human epigenetic signaling (29, 30). The G9aKme is targeted by the HP1 chromodomain in one transcriptional co-repressor complex (30). Interestingly, the human CDYL protein was also found associated with G9aKme in pulldown experiments from cellular extracts.

Because methylation of lysine residues within numerous ARK(S/T) motifs appears to orchestrate complex epigenetic pathways (for review, see Refs. 29, 32–34), determining the specificity of effectors may be a paradigm for understanding epigenetic signaling. Using a series of *in vitro* and cell-based assays, we studied the biochemical specificity of the chromodomains in the CDY family proteins. Our studies reveal a surprising variability in discriminatory interactions of CDY and CDYL2 chromodomains with methylated ARK(S/T) motifs.

EXPERIMENTAL PROCEDURES

Antibodies—Polyclonal antibodies specific for H3K9me3 were a gift from Dr. Thomas Jenuwein (IMP Vienna). The monoclonal antibody against mouse HP1α was obtained from Chemicon, and the monoclonal anti-FLAG antibody was purchased from Sigma.

Peptide Preparation—The sequences of the synthetic peptides corresponding to histone tails are listed below. A non-native tyrosine residue at the C terminus of each peptide was used for concentration determination by UV absorption measurements. Peptides were labeled with fluorescein as previously described (13):

H3K9me1, H3K9me2, H3K9me3: NH_2-ARTKQTARK-(me)STGGKAY-COOH; H3K27me, H3K27me2, H3K27me3: NH_2-APRKQLATQAARK(me)SAPSTY-COOH; H3tK27me3: NH_2-APRKQLATQVARK(me)SAPSTY-COOH; H1.4K26-me3: NH_2-TPVKKKARK(me)SAGAAKY-COOH; H3K9me3-S10ph: NH_2-ARTKQTARK(me)S(ph)TGGKAY-COOH; H3K27-me3S28ph: NH_2-APRKQLATQAARK(me)S(ph)APSTY-COOH; H3K9ac: NH_2-ARTKQTARK(ac)STGGKAY-COOH; H3K4me3, NH_2-ARTK(me3)QTARKSTGGKAY-COOH; H3K4me2K9me2: NH_2-ARTK(me2)QTARK(me2)STGGKAY-COOH; G9aKme3, G9aKme1: NH_2-QPKVHRARK(me)TMSKPGY-COOH; unmodified H3(1–15): NH_2-ARTKQTARKSTGGKAY-COOH; unmodified H3(15–32): NH_2-APRKQLATQVARKSAPSTY-COOH; unmodified H1.4(18–32): NH_2-TPVKKKARKSAGAAKY-COOH; unmodified G9a, NH_2-QPKVHRARKTMSKPGY-COOH.

Molecular Biology—For binding studies, the chromodomains of human CDY (GenBank^{TM} AF000981; residues 1–78), human CDYL (GenBank^{TM} AF081259; residues 1–133, 58–133, or 60–133), mouse CDYL (GenBank^{TM} AF081261; residues 1–128 or 51–128), and mouse CDYL2 (GenBank^{TM} AK015452; residues 1–75) were amplified by PCR and cloned into the BamHI/NdeI sites of the pET16b vector (Novagen). Full-length CDY and CDYL2 were cloned into a modified pMAL vector (New England Biolabs) for expression as MBP-His fusion proteins (details are available upon request). To generate C-terminal epitope-tagged constructs for the transient expression of full-length human CDY and human CDYL, we used PCR amplification with reverse primers containing the sequence encoding for the FLAG and hemagglutinin peptides (for details, see Ref. 47). cDNAs were cut with the appropriate restriction enzymes and cloned into the BamHI/XbaI sites of the pcDNA3.1+ vector (Invitrogen). Site-directed mutagenesis was performed according to the QuikChange protocol (Stratagene).

Fluorescence Polarization Binding Assays—Fusion proteins with the N-terminal His tag were expressed in *Escherichia coli* strain BL21(DE3) (Novagen) and purified by Ni^{2+}-affinity chromatography (Qiagen) and gel filtration chromatography (Superdex 75 resin, GE Healthcare). N-terminal MBP-His fusion proteins of full-length CDY and CDYL2 were expressed in BL21 RIL (Novagen) and purified consecutively on maltose and nickel-nitrilotriacetic acid resins. Protein concentrations were determined by absorbance spectroscopy using predicted extinction coefficients (for CDY chromodomain ϵ_{280} = 19,750 $M^{-1}cm^{-1}$; for MBP-His-CDY ϵ_{280} = 113,000 $M^{-1}cm^{-1}$; for CDYL chromodomain ϵ_{280} = 15,220 $M^{-1}cm^{-1}$; for CDYL2 chromodomain ϵ_{280} = 20,910 $M^{-1}cm^{-1}$; for MBP-His-CDYL2 ϵ_{280} = 126,000 $M^{-1}cm^{-1}$). Peptide concentrations were determined using absorbance spectroscopy (extinction coefficient for tyrosine, ϵ_{280} = 1280 $M^{-1}cm^{-1}$; extinction coefficient for fluoresceinated peptides ϵ_{492} = 68,000 $M^{-1}cm^{-1}$). Fluorescence polarization binding assays were performed under conditions of 20 mM imidazole, pH 8.0, 25 mM NaCl, 2 mM dithiothreitol and in the presence of 100 nM fluorescein-labeled peptide following a previously described protocol (13). Data were obtained using a Teacan Polarion 96-well plate reader or a Hidex Chameleon II plate reader (100 flashes). Sample plates were kept on ice until fluorescence reading at room temperature. Titration binding curves were analyzed using KaleidaGraph (Synergy Software) as previously described (13).

Isothermal Titration Calorimetry—Isothermal titration calorimetry (ITC) experiments were carried out as described previously using a VP-ITC instrument (MicroCal) (13). Chromodomains of CDY or HP1 were dialyzed against 50 mM sodium phosphate, pH 8.0, 25 mM NaCl, and 2 mM dithiothreitol. Peptides were purified by gel filtration in water (G10 resin, GE Healthcare), lyophilized, and dissolved in the chromodomain dialysis buffer. Exothermic heats of reaction (μcal/s) were measured at the indicated temperatures by automated sequencing of 30 injections of the H3 peptides (750 μM), each 10 μl, spaced at 2-min intervals, into 1.41 ml of chromodomain (CDY at 60 μM; HP1 at 70 μM). Binding curves were analyzed by non-linear least squares fitting of the data using the Origin (MicroCal) software package.

Cell Transfection—NIH3T3 (American Cell Culture Collection) and mouse embryonic fibroblast (a kind gift of Dr. Thomas Jenuwein, IMP Vienna) cells were grown at 37 °C in a humidified atmosphere, 5% CO_2 using Dulbecco's modified Eagle's medium (Invitrogen) supplemented with 10% fetal

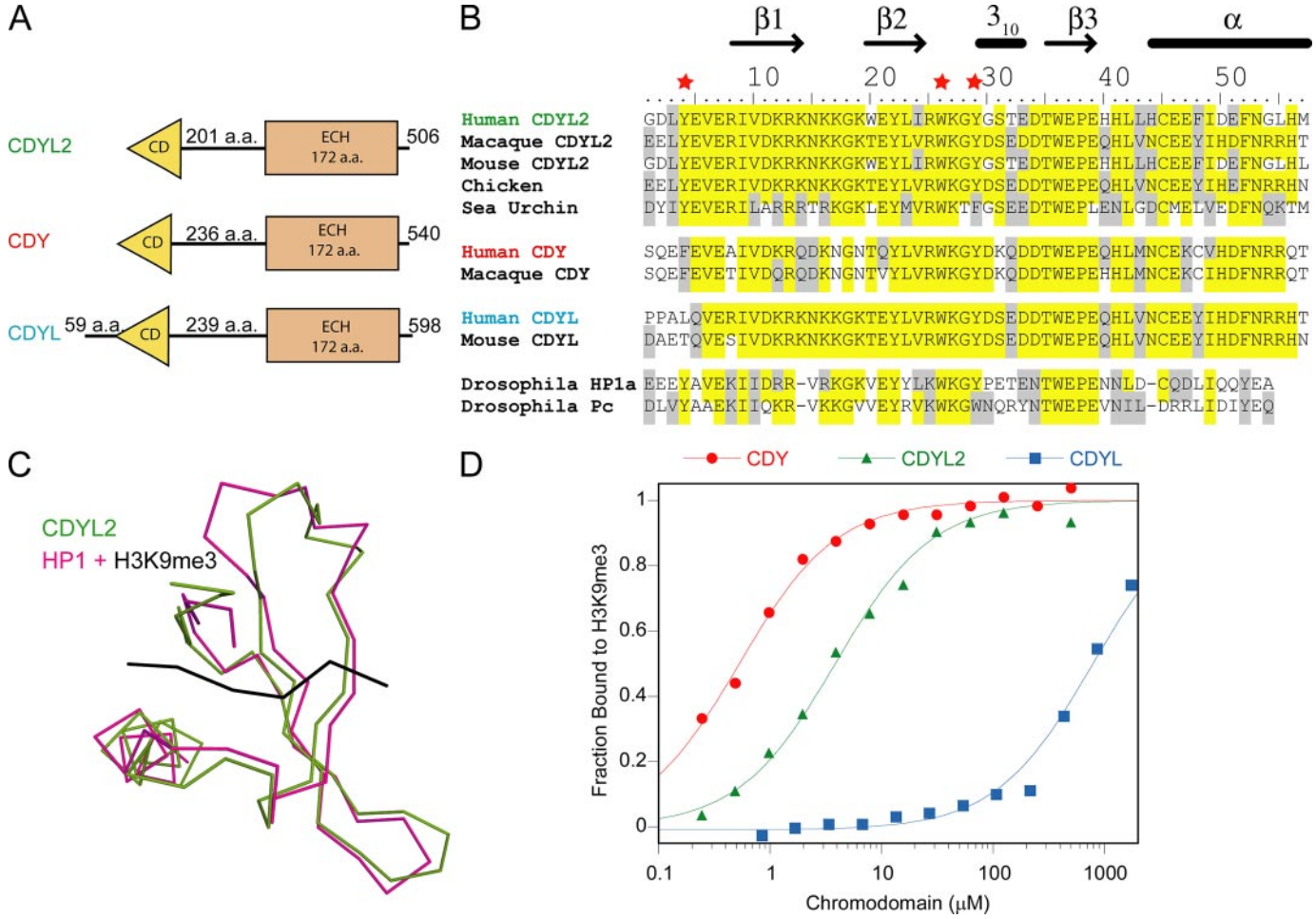

FIGURE 1. **The CDY protein family and their chromodomains.** *A*, schematic representation of the primary structures of CDYL, CDYL2, and CDY. *a.a.*, amino acids. *B*, sequence alignment of CDY family chromodomains, which are related to HP1 and Polycomb chromodomains. *Three stars above* the *sequence mark* the positions of the aromatic cage residues. Secondary structure elements above the sequence correspond to that deduced for CDYL2 (from PDB code 2dnt). The accession codes are: human CDY, Q9Y6F8; Macaque CDY, AJ31484;, human CDYL, Q9Y232; mouse CDYL, Q9WTK2; human CDYL2, AK096185; Macaque CDYL2, AY271718; mouse CDYL2, AK015452; chicken CDYL2, XP_418964; sea urchin CDYL2, XP 781347. *C*, backbone superposition of the three-dimensional structure of the human CDYL2 chromodomain (*green*, from PDB code 2dnt) on the structure of the *Drosophila* HP1 (from PDB code 1kne) chromodomain (*pink*) bound to an H3K9me3 peptide (*black*). *D*, interaction of recombinant human CDY family chromodomains with an H3K9me3 peptide as measured by fluorescence polarization. Averages from at least three independent measurements are plotted. See Table 1 for dissociation constants.

bovine serum, 2 mM glutamine. Cells were transfected using Lipofectamine 2000 as instructed by the manufacturer (Invitrogen).

Immunofluorescence—For immunofluorescence staining, cells were grown and transfected on glass coverslips. 48 h post-transfection, cells were fixed in solution I (1× PBS, 3.7% formaldehyde, 1% Triton X-100, 2% Nonidet P-40) for 10 min and then washed in 1× PBST (PBS, 1% Triton X-100) for 3 × 10 min. Slides were blocked for 1 h (1× PBST, 5% goat serum, 2% bovine serum albumin) and incubated with the indicated primary antibodies overnight in a humidified atmosphere. Dilutions for primary antibodies were anti-H3K9me3 (1:1500), anti-HP1α (1:2000), and anti-FLAG (1:500). Slides were washed in 1×PBST for 3 × 10 min and incubated with the appropriate secondary antibodies (Molecular Probes, Jackson ImmunoResearch) for 2 h in a humidified atmosphere. After washing in 1× PBST, DNA was stained with DAPI (1 μg/ml) for 10 s. Pictures were taken on a Leica SP5 confocal microscope or a Zeiss Axiopod II both equipped with 60× lenses.

RESULTS

Variability in Binding to H3 Methylated on Lys-9—The CDY class of chromodomains exhibits high homology to HP1 and Polycomb chromodomains (Fig. 1*B*). Three aromatic residues were shown to be necessary for assembling a methyllysine binding aromatic cage in HP1 and Polycomb chromodomains (11, 12, 16). Interestingly, the chromodomains of the CDYL proteins do not have the first aromatic cage residue, suggesting substantial difference in the function of this factor. A three-dimensional structure corresponding to the chromodomain of CDYL2 has been deposited in the protein data bank (PDB accession code 2dnt). We prepared a superposition of the CDYL2 structure with the peptide-bound structure of the HP1 chromodomain involving an H3K9me3 peptide (11) (Fig. 1*C*). This comparison established that CDYL2 and, by homology, CDY and CDYL chromodomains, despite a moderate sequence identity (~42%), have tertiary structures similar to HP1. Whereas HP1 and Polycomb chromodomains are 50-residue modules, the CDY family chromodomains are 55-residue mod-

ules containing a longer C-terminal α-helix (Fig. 1*B*). Previously, binding of the CDY chromodomain to H3K9me2 and H3K9me3 peptides was identified through protein microarray analysis (7).

To determine the specificity and affinity for methylated histone lysine residues among the three CDY family members, recombinant chromodomains of CDY, CDYL, and CDYL2 were expressed in bacteria and purified. Because the CDYL chromodomain has an incomplete aromatic cage plus an N-terminal extension (Fig. 1, *A* and B), we prepared a recombinant construct that included the N terminus of the protein together with the chromodomain module. Recombinant proteins were used in fluorescence polarization assays to measure equilibrium binding to fluoresceinated synthetic peptides corresponding to the histone H3 tail. The binding data are shown in Fig. 1*D*, and the dissociation constants are listed in Table 1. In accordance with sequence prediction and the presence of an incomplete aromatic cage, we measured no binding of the CDYL chromodomain to H3K9me3 ($K_D > 500$ μM). Surprisingly, we measured a substantial difference in the dissociation constants associated with CDY and CDYL2. The interaction of the CDY chromodomain with the H3K9me3 peptide is 8-fold stronger than that of CDYL2. The results confirm subtle sequence differences among CDY family chromodomains, impacting on their interaction with methylated histone tails. The binding studies potentially implicate each CDY family member as part of distinct chromatin modification pathways.

TABLE 1
Dissociation constants (μM) measured by fluorescence polarization for CDY family chromodomains interacting with synthetic peptides as described under "Experimental Procedures"

Peptide	CDY	CDYL	CDYL2
H3 Lys-9			
Unmodified	~300	>500	>500
H3K4me3	~300	>500	>500
H3K9ac	~300	>500	>500
H3K9me1	3.4 ± 0.5	>500	67 ± 10
H3K9me2	0.7 ± 0.1	>500	8.9 ± 1.1
H3K9me3	0.5 ± 0.1	452 ± 81	3.9 ± 0.5
H3K4me2K9me2	0.9 ± 0.2	~500	11.0 ± 2.1
H3K9me3S10ph	38 ± 4	>500	>500
H3 Lys-27			
Unmodified	>500	>500	>500
H3K27ac	>500	>500	>500
H3K27me1	~300		113 ± 15
H3K27me2	119 ± 37		18.4 ± 3.1
H3K27me3	76 ± 11	>500	12.4 ± 1.2
H3K27me3S28ph	>500		>500
Testis H3 Lys-27			
H3tK27me3	7.5 ± 0.8	~500	2.6 ± 0.4
H1.4 Lys-26			
Unmodified	>500	>500	>500
H1.4K26me3	10 ± 1	~500	2.2 ± 0.4
G9a Lys-185			
Unmodified	185 ± 17	>500	>500
G9a-K185me1	36 ± 9	>500	108 ± 27
G9a-K185me3	0.6 ± 0.2	~500	4.9 ± 1.2

Distinct in Vivo Distribution of CDY, CDYL, and CDYL2 Proteins—Given the CDYL chromodomain does not bind to the H3K9me3 peptide and the CDY chromodomain binds more avidly than the CDYL2 chromodomain, we investigated the *in vivo* localization of these proteins in relation to heterochromatin in mammalian systems. We made use of mouse fibroblast cells (NIH3T3 and MEF cells) that show a distinct pattern of DNA-dense, pericentromeric heterochromatin regions in the nucleus. These coincide with local enrichment of H3K9me3 modification. The distribution of CDY family proteins in these cells was compared using transiently expressed fusion constructs that encode their full-length polypeptides with a C-terminal FLAG tag. As Fig. 3 shows, all three fusion proteins displayed an exclusively nuclear distribution (see also supplemental Fig. S1).

In all cells inspected, we detected the transiently expressed CDY protein excluded from the nucleoli and enriched at the many large DAPI-dense regions reminiscent of the endogenous HP1α protein (17) (supplemental Fig. S2). Previously, Kim *et al.* (7) also showed CDY and

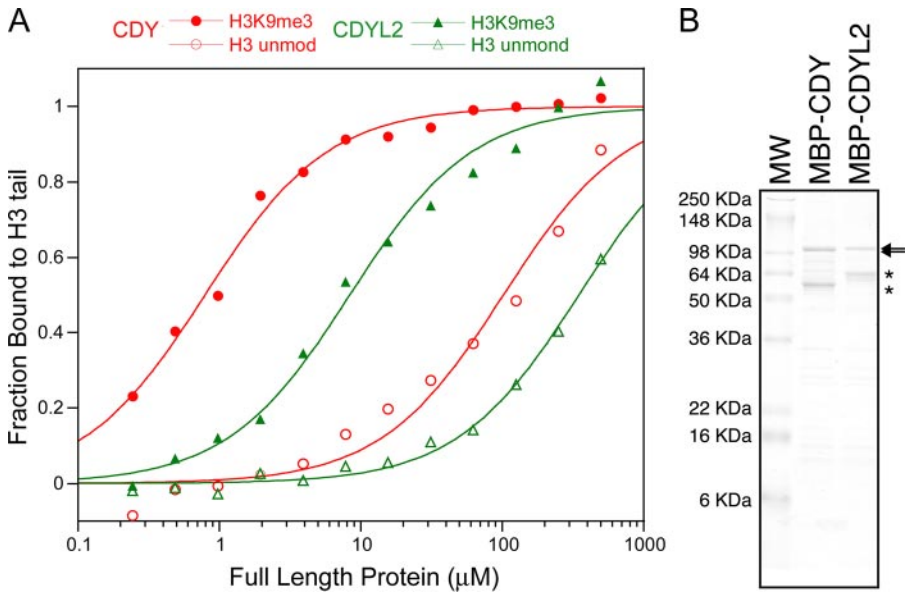

FIGURE 2. **Interaction with methylated lysine residues is an intrinsic property of CDY family proteins.** *A*, interaction of recombinant full-length human CDY and mouse CDYL2 proteins fused to MBP with an H3K9me3 or the corresponding unmodified peptide as measured by fluorescence polarization. Averages from at least three independent measurements are plotted. *B*, recombinant MBP fusion proteins used for the measurements in *panel A* were run on SDS-PAGE gels and stained with Coomassie Blue. *Arrows* indicate the MBP-CDY and MBP-CDYL2 recombinant proteins. Major degradation products co-purifying with the recombinant proteins are indicated. Molecular weight (*MW*) markers are shown on the *left*.

HP1β exhibit overlapping distributions in chromatin with the H3K9me3 modification. Although the transiently expressed CDYL protein was also excluded from the nucleoli, CDYL showed a diffuse distribution pattern that never overlapped with regions of H3K9me3 (Figs. 3*B* and supplemental Fig. S2*B*). Interestingly, the CDYL2 protein was found throughout the nucleus in a punctate distribution pattern with pronounced cell-to-cell variation. Whereas some nuclei displayed granular staining of CDYL2, others showed larger areas of CDYL2 enrichment (Figs. 3*C* and supplemental Fig. S3*C*). Although CDYL2 enrichment at DAPI dense regions was less pronounced as compared with CDY, all cells analyzed exhibited some CDYL2 co-localized with regions of H3K9me3. Together, these observations underscore substantial differences in chromatin recognition and binding of the CDY family proteins.

CDY and CDYL2 Are Differentially Sensitive to the Degree of Lysine Methylation—The level of methylation (mono-, di-, or trimethylation) of lysine residues in histone tails is important for chromatin regulation (10, 35). We, therefore, measured the binding affinities of CDY and CDYL2 as a function of the methylation level on H3K9. Previous studies as well as data listed in Table 2 indicate that the HP1 chromodomain exhibits 2–3-fold reduced interaction with H3K9me2 peptide as compared with H3K9me3 peptide, whereas the binding to H3K9me1 peptide is substantially weaker. We found CDYL2 to resemble these features in HP1 (Table 1). However, the CDY chromodomain showed 20-fold stronger binding to H3K9me1 as compared with CDYL2. Interestingly, the binding of CDY to the H3K9me1 peptide is as efficient as the binding of CDYL2 or HP1 to the H3K9me3 peptide (Tables 1 and 2).

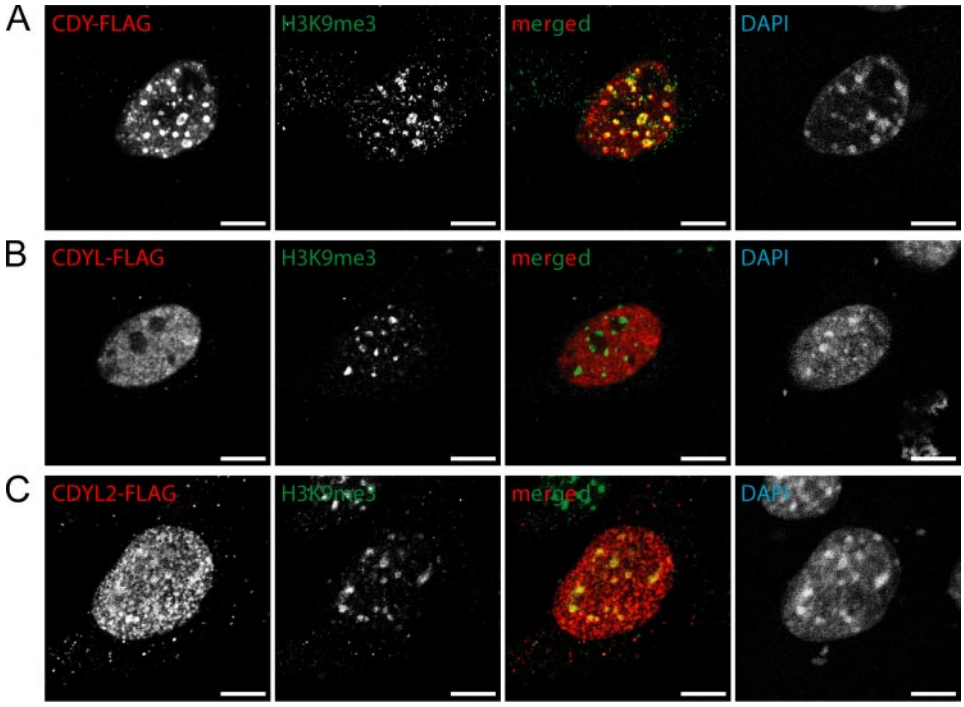

FIGURE 3. **Differential nuclear distribution of CDY family proteins.** FLAG-tagged human CDY (*A*), human CDYL (*B*), or mouse CDYL2 (*C*) were transiently expressed in NIH3T3 cells. Immunostaining with anti-FLAG-specific antibodies (*green*) and anti-H3K9me3 (*red*)-specific antibodies was analyzed by confocal microscopy. The merged image corresponds to the overlay of the two color channels. *Yellow areas* indicate colocalization sites for CDY family proteins with H3K9me3 modification. Cells of medium expression level representative for the nuclear distribution of the CDY family proteins are shown (see supplemental Fig. S1 for more images). DNA inside the cell nucleus was stained with DAPI and defines areas of high DNA density that are presumed to be heterochromatic. *Scale bar*, 10 μm.

To determine the thermodynamic basis for the unusually strong binding of CDY to the methylated H3 tail, we performed isothermal titration calorimetry. We studied the chromodomains of CDY and *Drosophila* HP1 proteins under identical solution conditions (Table 2). These measurements showed CDY binds the H3K9me3 peptide 8-fold stronger than HP1. The free energy of binding to the H3 tail is more favorable for CDY by 1.2 kcal/mol. Isothermal titration calorimetry measurements of CDY binding to the H3K9me3 peptide at five different temperatures allowed us to estimate the heat capacity of binding ($\Delta C_p = -0.22$ kcal/mol·K). The small ΔC_p suggests negligible conformational changes occur in the CDY chromodomain upon binding to the H3 tail, a result in close agreement with that found for *Drosophila* HP1 (11, 36).

Using calorimetry, we found the enthalpy of binding to the H3K9me3 peptide is substantially more favorable for CDY than for HP1. This finding emphasizes the

TABLE 2

Thermodynamic parameters for binding to H3 peptides methylated on Lys-9

Isothermal titration calorimetry analysis of the human CDY chromodomain is compared with the *Drosophila* HP1α chromodomain under identical solution conditions.

Protein	Peptide	T	K_D	ΔH	N	ΔG	$T\Delta S$
		°C	μM	kcal/mol		kcal/mol	kcal/mol
CDY	H3K9me3	5	0.11 ± 0.03	−11.83 ± 0.04	0.97	−8.61	−3.22
CDY	H3K9me3	10	0.14 ± 0.05	−12.62 ± 0.03	0.96	−8.54	−4.08
CDY	H3K9me3	15	0.30 ± 0.07	−13.69 ± 0.03	1.00	−8.59	−5.10
CDY	H3K9me3	20	0.35 ± 0.11	−14.99 ± 0.04	0.99	−8.57	−6.42
CDY	H3K9me3	25	0.73 ± 0.17	−16.19 ± 0.04	1.02	−8.53	−7.66
CDY	H3K9me2	15	0.86 ± 0.16	−17.21 ± 0.04	1.03	−8.23	−8.98
CDY	H3K9me1	15	7.86 ± 1.1	−17.70 ± 0.04	1.18	−6.38	−11.32
HP1	H3K9me3	16	2.3 ± 0.1	−9.71 ± 0.04	1.02	−7.36	−2.46
HP1	H3K9me2	16	6.9 ± 0.2	−9.47 ± 0.04	1.02	−6.78	−2.69
HP1	H3K9me1	16	31.3 ± 0.5	−7.75 ± 0.03	1.04	−5.92	−1.81

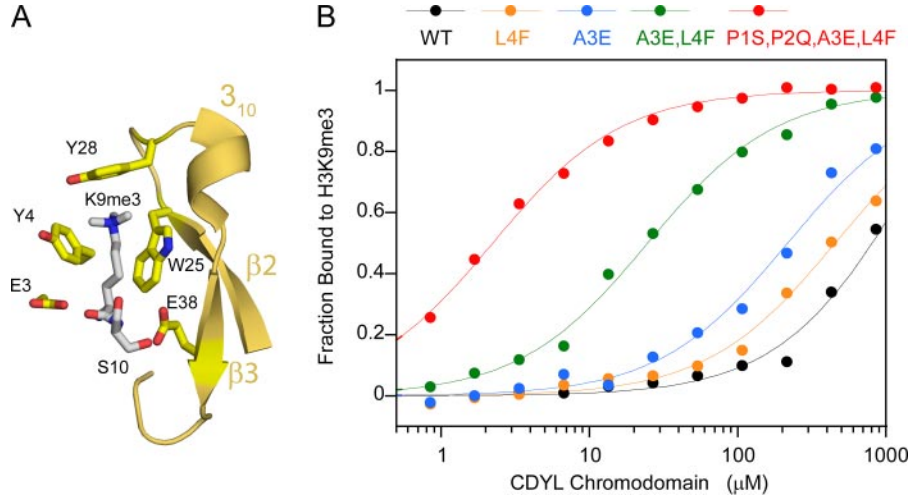

FIGURE 4. **Point mutations rescue CDYL H3K9me3 binding.** *A*, close-up view of the aromatic cage and surrounding secondary structure elements of the HP1 chromodomain interacting with H3K9me3 (PDB code 1kne). The side chains of E3 and E38 form hydrogen bonds with the backbone of the H3 tail and are solvent-exposed. Residues are numbered according to the sequence alignment in Fig. 1*B*. *B*, fluorescence polarization analysis of wild-type (*WT*) and mutant human CDYL chromodomains interacting with an H3K9me3 peptide. Averages from at least three independent measurements are plotted.

ability of CDY to establish more favorable polar interactions with the H3 tail than those used by HP1. Previous studies have shown that recognition of methyllysine by the HP1 chromodomain is driven by cation-π interactions between the methylated ammonium group of methylated H3K9 and the side chains of three aromatic residues (11, 16). The magnitude of the cation-π interaction depends on the electron density of the aromatic ring, which can substantially vary from a tyrosine to a phenylalanine as well as the degree of solvent exposure in the interaction site (37, 38). Whereas both CDYL2 and HP1 have a tyrosine at the first position of the aromatic cage, this position in CDY is substituted with a phenylalanine residue (Fig. 1*B*). Interestingly, this phenylalanine residue in CDY is further positioned between two polar (glutamic acid) residues that appear to improve solvent exposure of the aromatic cage. Together, these observations suggest that subtle amino acid changes surrounding the aromatic cage can lead to substantial differences in the strength of the cation-π interactions between chromodomains and methylated lysine residues.

CDY and CDYL2 Respond to a Binary Switch—A binary switch mechanism has been associated with the simultaneous presence of the H3K9me3 and H3S10ph modifications on the same histone tail (H3K9me3S10ph) (19, 20). Human HP1 variants are unable to interact with chromatin during mitosis because of the overwhelming presence of serine 10 phosphorylation (17, 18). In addition to its relevance to mitosis, H3S10ph is associated with transcriptionally active chromatin (10). To investigate the response of CDY and CDYL2 to such a binary switch, we performed additional fluorescence polarization binding assays. We found that both CDY and CDYL2 chromodomains are sensitive to the presence of H3S10ph. The binding to the H3K9me3S10ph peptide is 76-fold weaker for CDY and 100-fold weaker for CDYL2 as compared with binding to the H3K9me3 peptide (Table 1).

CDY and CDYL2 Chromodomains Bind to a Similar Fragment of the H3 Tail—The comparison of the structure of the CDYL2 chromodomain with that of HP1 suggests that H3 tail residues 5 through 10 should be sufficient for binding to CDY and CDYL2 chromodomains (11) (Fig. 1*C*). The interaction of CDY and CDYL2 chromodomains with the H3 tail involves one residue C-terminal to the methyllysine, serine 10. As discussed above, serine 10 phosphorylation has a major impact on binding affinity. To determine to what extent residues N-terminal to the methyllysine could impact on CDY and CDYL2 interaction with the H3 tail, we tested the influence of an adjacent modification on binding affinity, the presence of methylation at H3K4. We performed additional fluorescence binding assays using a peptide with simultaneous dimethylations at H3K4 and H3K9 (H3K4me2K9me2 peptide). As listed in Table 1, binding of CDY and CDYL2 chromodomains to the H3K4me2K9me2 peptide is nearly the same as interaction with H3K9me2, ~1.2-fold weaker. This finding suggests residue 4 of the H3 tail (position n-5) does not impact on the binding of CDY and CDYL2 to the H3 tail, similar to what has been observed for the interaction of *Drosophila* HP1 with the H3 tail (11).

Point Mutations Rescue CDYL Binding to the H3 Tail—Table 2 shows that we could not measure appreciable binding of the CDYL chromodomain to any methylated H3K9 peptide or the unmethylated peptide. We speculated that the critical contributing factor might be the absence of one of the residues in the aromatic cage (Fig. 1*B*). Given the 70% sequence identity between CDYL and CDY, we asked whether the H3 tail could bind to CDYL using alternate histone H3 modifications. We concentrated on methylated H3K4 (H3K4me3) and acetylated H3K9 (H3K9ac) modifications, as both modifications are found associated with the histone H3.3 variant within transcriptionally active chromatin. As shown in Table 1, we found no appreciable binding of CDYL to either of these peptides. We then asked whether the N-terminal extension of the chromodomain in CDYL could interfere with binding interactions. By preparing a separate recombinant construct of human CDYL that excluded the N-terminal extension, we measured the affinity for methylated and unmethylated H3 peptides again and observed no substantial differences (data not shown). The corresponding recombinant chromodomain of the mouse CDYL also did not bind to the H3K9me3 peptide (data not shown).

We then asked whether we could establish efficient binding of the CDYL chromodomain to the H3K9me3 peptide by using site-directed mutagenesis. We used the CDY sequence as a guide to prepare point mutations in CDYL. To restore the aromatic cage, we prepared a Leu-61 to Phe mutant (position 4 in the chromodomain; Figs. 1*B* and 4*A*). This mutant exhibits negligible improvement in binding affinity for the H3K9me3 peptide (Fig. 4*B* and Table 3). In the structure of the complex of HP1 with the H3 tail, the side chain of the residue preceding the

TABLE 3

Dissociation constants (μM) measured by fluorescence polarization for recombinant mutant CDYL chromodomains interacting with synthetic peptides as described under "Experimental Procedures"

Peptide	Wild type	A3E	L4F	A3E,L4F	P1S,P2Q,A3E,L4F
H3 Lys-9					
Unmodified	>500	>500	>500	>500	>500
H3K4me3	>500	>500	>500	>500	>500
H3K9ac	>500	>500	>500	>500	>500
H3K9me1	>500	240 ± 60	>500	55 ± 10	13 ± 2
H3K9me2	>500	186 ± 24	~500	33 ± 8	3.4 ± 0.5
H3K9me3	>500	216 ± 31	452 ± 81	25 ± 11	2.2 ± 0.3
H3K4me2K9me2	>500	177 ± 33	~500	41 ± 7	3.5 ± 0.4
H3K9me3S10ph	>500	>500	>500	>500	>500
H3 Lys-27					
Unmodified	>500	>500	>500	>500	>500
H3K27ac	>500	>500	>500	>500	>500
H3K27me3	>500	323 ± 41	>500	101 ± 17	23 ± 5
Testis H3 Lys-27					
H3TK27me3	>500	225 ± 22	~500	38 ± 8	13 ± 3
H1.4 Lys-26					
Unmodified	>500	>500	>500	>500	100 ± 24
H1.4K26me3	>500	500 ± 71	~500	81 ± 12	6.5 ± 1.9
G9a Lys-185					
Unmodified	>500	>500	>500	>500	>500
G9aK185me3	>500	182 ± 31	~500	37 ± 7	40 ± 10
G9aK185me1	>500	271 ± 53	>500	52 ± 19	19 ± 3

first aromatic residue is a Glu (position 3 in the chromodomain), which forms intermolecular hydrogen bond with the backbone of Lys 9 (Fig. 4*A*). Glu-3 also improves solvent exposure at the binding pocket of the HP1 chromodomain. Because this residue is substituted with an Ala in human CDYL, we tested the effect of an Ala to Glu mutation for binding to the H3K9me3 peptide and measured a small but noticeable improvement in binding (factor of 3) (Fig. 4*B*). Subsequently, we prepared a double mutant of CDYL with substitutions at both positions 3 and 4 of the chromodomain and found a synergistic effect (30-fold improvement in binding) (Fig. 4*B*, Table 3).

Because the mutation of the CDYL chromodomain residue 3 exhibited a synergistic effect with the addition of the aromatic residue 4, we hypothesized mutations at residues 1 and 2 may further improve solvent exposure of the peptide binding pocket, impacting cation-π interactions. Therefore, we prepared four simultaneous mutations in CDYL to convert residues 1–4 to those of the CDY chromodomain (P1S,P2Q,A3E,L4F, Fig. 1*B*). This mutant CDYL exhibited a further 10-fold improvement in binding to the H3K9me3 peptide (Fig. 4*B*, Table 3). As compared with CDY, this mutant CDYL bound only 4-fold weaker to the H3K9me3 peptide, yet the binding was 2-fold stronger than that measured for CDYL2.

To test the affinity of these CDYL mutants for H3K9me3 in a cell-based assay, we transiently expressed full-length CDYL polypeptides bearing the A3E,L4F and P1S,P2Q,A3E,L4F mutations in NIH3T3 cells. As Fig. 5 shows, both mutant proteins were exclusively localized to the cell nucleus and were excluded from the nucleoli as was the wild-type CDYL protein (Fig. 3*B*). Interestingly, the nuclear distribution of the mutant proteins in relation to the DAPI dense areas and regions of pericentric heterochromatin with H3K9me3 varied among different cells. Three types of localization patterns for CDYL mutants could be observed (Fig. 5*C*). In a substantial number of cells, both mutants showed diffuse staining (type I) that was excluded from pericentromeric heterochromatin and is reminiscent of the wild-type CDYL protein (Figs. 3*B* and 5). Interestingly, in some cells the A3E,L4F mutant CDYL showed some overlap with DAPI dense regions and H3K9me3 modification as indicated by the yellow areas in the merged images (type II). Although the P1S,P2Q,A3E,L4F mutant CDYL exhibited both type I and type II localization patterns, it also showed punctate overlap with pericentromeric heterochromatin (type III), reminiscent of the CDY protein (Fig. 3*A*). Overall, the gradual changes in subnuclear localization observed support the biochemical function of these point mutations.

Other Potential Binding Sites for CDY and CDYL2 in Chromatin—In addition to H3K9me3, other lysine-methylated ARK(S/T) motifs depicted in Fig. 6*A* may recruit CDY family chromodomains. Therefore, we measured dissociation constants for the binding of CDY, CDYL2, wild-type CDYL, and the mutant CDYL chromodomains to four additional peptides (Fig. 6*B*, Tables 1 and 3). We found the binding of the CDY chromodomain to H3K27me3 and H3tK27me3 peptides to be 150- and 15-fold weaker, respectively, than binding to the H3K9me3 peptide. Interaction of CDY chromodomain with the H1.4K26me3 peptide was also found to be 20-fold weaker than binding to the H3K9me3 peptide. Surprisingly, the CDY chromodomain bound to the G9a-K185me3 peptide with dissociation constant similar to that found for the H3K9me3 peptide (Fig. 6*B*). When we compared binding differences among monomethylated peptides, we found the dissociation constant for binding of CDY to H3K9me1 and G9a-K185me1 peptides are significantly different, 3.4 and 36 μM, respectively. Together, these results suggest the CDY chromodomain is capable of discriminating between various lysine-methylated ARK(S/T) motifs.

Interestingly, the CDYL2 and the mutant CDYL chromodomains are substantially less selective than the CDY chromodomain in binding to different ARK(S/T) motifs (Fig. 6*B*). Among the peptides tested, the H3K27me3 peptide showed the weakest

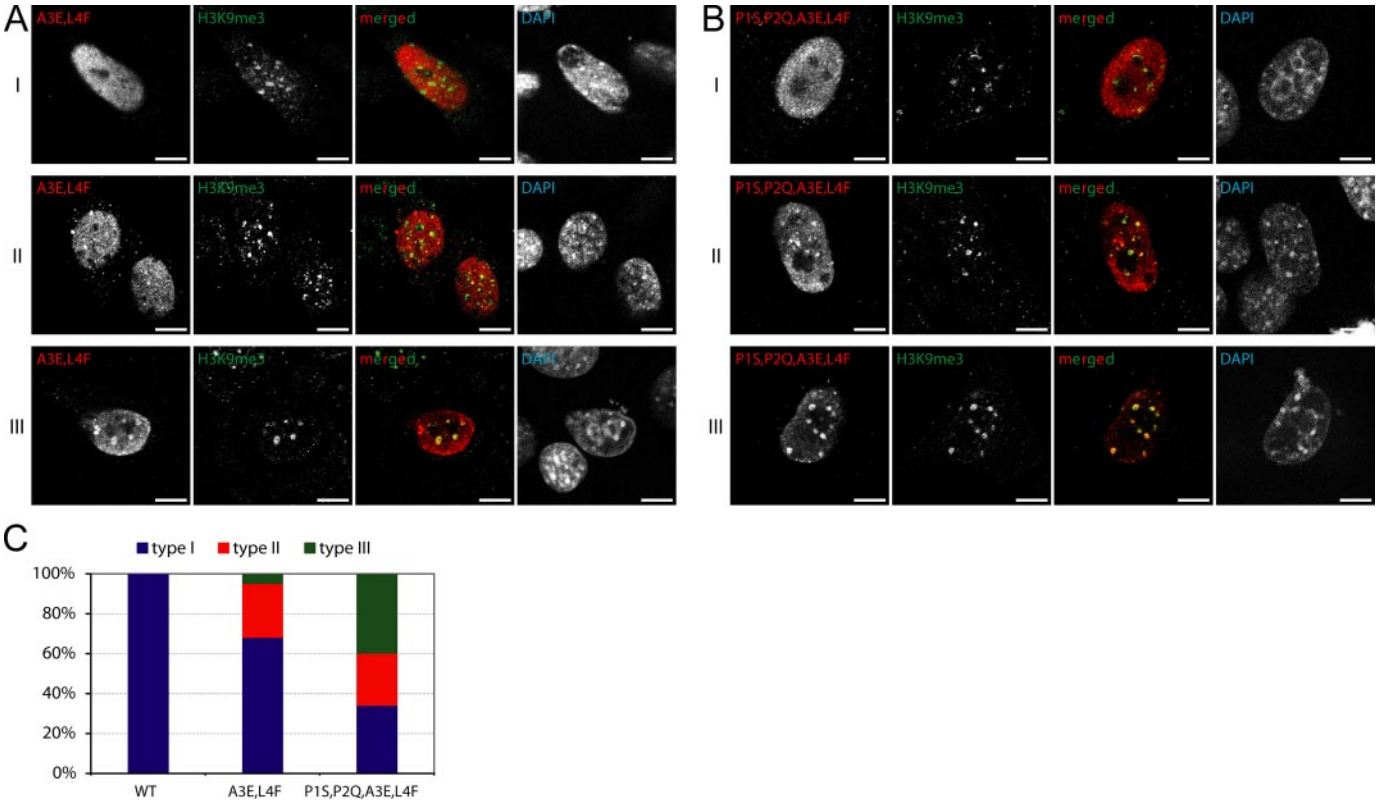

FIGURE 5. **CDYL mutant chromodomain H3K9me3 interaction is sufficient for localization to pericentromeric heterochromatin.** FLAG-tagged human CDYL chromodomain mutants A3E,L4F (*A*), and P1S,P2Q,A3E,L4F (*B*) were transiently expressed in NIH3T3 cells. Cells were immunostained and analyzed as described in Fig. 3. Cells of medium expression level representative for three different types (I-III) of nuclear distribution found for both mutants are shown. The *scale bar* is 10 μm. *C*, the occurrence of type I, II, or III nuclear distribution in each cell for wild-type CDYL (*WT*), CDYL A3E,L4F, and CDYL P1S,P2Q,A3E,L4F were statistically analyzed. Frequency plots resulting from the evaluation of at least 40 cells each from different transfection experiments are shown.

interaction for all CDY family chromodomains. Although the CDYL2 chromodomain exhibits similar binding to G9a-K185me3, H1.4K26me3, H3tK27me3, and H3K9me3 peptides, the mutant CDYL chromodomain is able to discriminate and bind strongly to the H3K9me3 peptide. The variability in dissociation constants listed in Tables 1 and 3 underscores the role of sequence differences in CDY family chromodomains for the specificity of their interactions with modified histone tails.

DISCUSSION

The expansion of HP1-like chromodomains in diverse proteins of higher eukaryotes suggests an increase in complexity of epigenetic regulatory pathways from lower to higher eukaryotes. The human genome contains the largest number of HP1-like chromodomains that are encoded by 16 different genes, and these encode proteins belonging to 5 different families, HP1, Suv91, Polycomb, CDY, and MPP8 (supplemental Fig. S3). Among these factors, HP1 and Suv91 are typically found associated with H3K9me3 regions of chromatin. The CDY and MPP8 families appear to be hallmarks of vertebrate genomes. The origin of their expansion into multiple variants is not well known. Previously, an evolutionary tree was delineated for the human CDY family genes, which suggested CDYL is the ancestor of CDY and CDYL2 (6). This would suggest that evolutionary forces first abolished methyllysine binding in an HP1-like chromodomain to formulate CDYL; subsequently methyllysine binding was gained in CDYL2 and CDY. This order of events is unlikely because the genomes of simple vertebrates like sea urchin or chicken encode only one CDY family gene whose sequence suggests full capability of binding to lysine-methylated ARK(S/T) motifs (Fig. 1*B*). Therefore, we assume CDYL2 is the ancestor of CDY and CDYL proteins.

The CDYL chromodomain is unable to bind to any lysine-methylated ARK(S/T) motif. We identified mutations in the CDYL chromodomain that can impact the interaction of the full-length protein with H3K9me3 regions of chromatin, suggesting its chromodomain is significant for cellular localization. Previous studies have implicated CDYL in transcriptional co-repressor complexes containing multiple chromatin modification enzymes and docking factors (39). Interestingly, the CDYL protein co-purified with the methylated G9a protein in human cell extracts (30). Together these results suggest the combined action of another factor could make up for the missing portion of the CDYL binding pocket. This may be related to a study on the yeast histone deacetylase complex Rpd3S, where the combined action of a PHD finger and a chromodomain from two different polypeptides has been suggested to regulate binding to H3K36me3 modification (40).

Although human CDY and CDYL2 chromodomains are able to recognize a variety of lysine-methylated ARK(S/T) motifs, there are substantial differences in their binding specificities. We found that the CDY chromodomain preferentially binds to the H3K9me3 peptide, whereas CDYL2 can equally interact

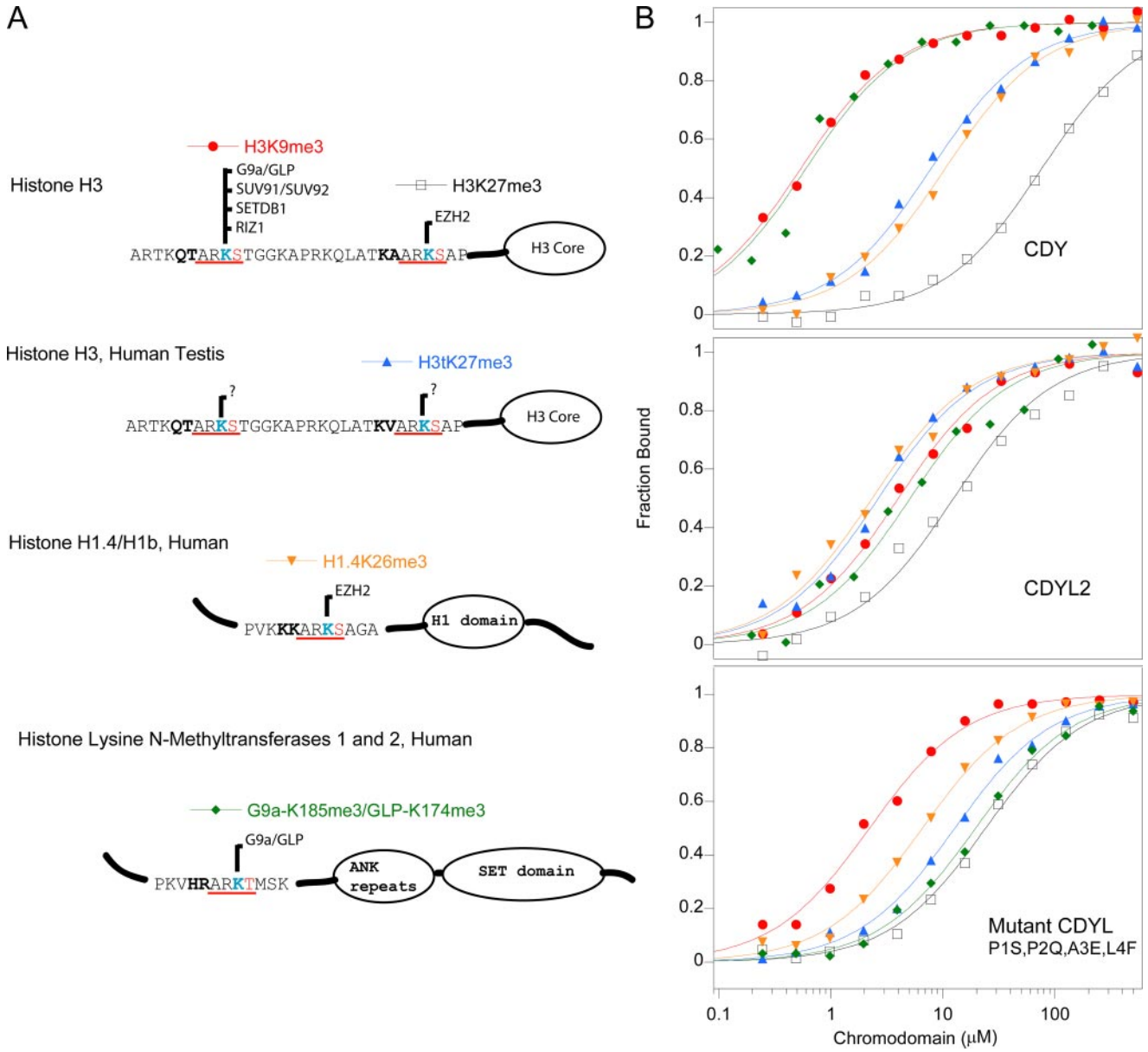

FIGURE 6. **Interaction of CDY family chromodomains with methyllysines embedded in ARK(S/T) motifs.** *A*, the ARK(S/T) motifs in chromatin that are potential binding sites of CDY family chromodomains are specified. The various methyltransferases that are known to establish the different methylations are listed *above each lysine residue*. *B*, fluorescence polarization binding assays were used to determine the specificities of the CDY, CDYL2, and CDYL P1S,P2Q,A3E,L4F chromodomains to each of these peptides containing a trimethyllysine. Averages from at least three independent measurements are plotted.

with H3K9me3, H3tK27me3, and H1.4K26me3 peptides. Studies on mouse polycomb (Pc) variants also showed substantial diversity in binding selectivity toward H3K9me3 and H3K27me3 (21). For example, Pc1 (Cbx2) showed equal binding to H3K9me3 and H3K27me3, whereas Pc2 (Cbx4) showed a 3-fold stronger binding to H3K9me3 (21). The mammalian Pc proteins are believed to contribute to chromatin architecture on the inactive X chromosome and reflect assembly of facultative heterochromatin using H3K9me3 and H3K27me3 modifications (21). The same chromatin modifications also seem to contribute to chromatin regulation during spermatogenesis (41, 42). Additional studies are required to determine how variability in methyllysine recognition by CDY, CDYL, and CDYL2 could impact on their functions in chromatin regulation in testis. Acetylation of histone H4 during spermatogenesis is suggested to hinge on the expression of CDY and CDYL, and these polypeptides are unique for their ability to link a repressive modification like H3K9me3 with that of histone H4 acetylation (8). Enrichment of CDY variants in testis might contribute to genomic imprinting, which leads to appropriate transcription of paternally derived genes (for review, see Refs. 31, 32, and 43). Unfortunately, at present only limited knowledge is available on the features of chromatin in human male germ cells.

Recently, we reported substantial evolutionary differences in the binding abilities of CHD double chromodomains that correlate with limited amino acid changes (44). These observations are consistent with complex control mechanisms associated with signaling enzymatic function in higher eukaryotes (45). In

both the CDY and CHD families of chromodomains, catalytic activity is physically separable from an N-terminal chromodomain that appears to link input or output signals associated with epigenetic regulation. Another role of the chromodomain may be direct participation in enzymatic activity. For example, studies on Suv91 (supplemental Fig. S3) showed deletion of the chromodomain or point mutations in the aromatic cage impaired enzyme activity (*i.e.* trimethylation of H3K9) despite the presence of an intact catalytic SET domain (46). Additional studies are necessary to further dissect the catalytic function of CDY family ECH domains and subsequently investigate whether their chromodomains directly participate in enzymatic activity and/or serve to link with input/output signaling networks.

Acknowledgments—We thank Judd Rice for performing anti-mouse HP1α immunostainings and Thomas Jenuwein for providing anti-H3K9me3 antibodies and mouse embryonic fibroblast cells used in our studies.

REFERENCES

1. Lahn, B. T., and Page, D. C. (1997) *Science* **278,** 675–680
2. Skaletsky, H., Kuroda-Kawaguchi, T., Minx, P. J., Cordum, H. S., Hillier, L., Brown, L. G., Repping, S., Pyntikova, T., Ali, J., Bieri, T., Chinwalla, A., Delehaunty, A., Delehaunty, K., Du, H., Fewell, G., Fulton, L., Fulton, R., Graves, T., Hou, S. F., Latrielle, P., Leonard, S., Mardis, E., Maupin, R., McPherson, J., Miner, T., Nash, W., Nguyen, C., Ozersky, P., Pepin, K., Rock, S., Rohlfing, T., Scott, K., Schultz, B., Strong, C., Tin-Wollam, A., Yang, S. P., Waterston, R. H., Wilson, R. K., Rozen, S., and Page, D. C. (2003) *Nature* **423,** 825–837
3. Hughes, J. F., Skaletsky, H., Pyntikova, T., Minx, P. J., Graves, T., Rozen, S., Wilson, R. K., and Page, D. C. (2005) *Nature* **437,** 100–103
4. Kuroda-Kawaguchi, T., Skaletsky, H., Brown, L. G., Minx, P. J., Cordum, H. S., Waterston, R. H., Wilson, R. K., Silber, S., Oates, R., Rozen, S., and Page, D. C. (2001) *Nat. Genet.* **29,** 279–286
5. Kleiman, S. E., Yogev, L., Hauser, R., Botchan, A., Bar-Shira Maymon, B., Schreiber, L., Paz, G., and Yavetz, H. (2003) *Hum. Genet.* **113,** 486–492
6. Dorus, S., Gilbert, S. L., Forster, M. L., Barndt, R. J., and Lahn, B. T. (2003) *Hum. Mol. Genet.* **12,** 1643–1650
7. Kim, J., Daniel, J., Espejo, A., Lake, A., Krishna, M., Xia, L., Zhang, Y., and Bedford, M. T. (2006) *EMBO Rep.* **7,** 397–403
8. Lahn, B. T., Tang, Z. L., Zhou, J., Barndt, R. J., Parvinen, M., Allis, C. D., and Page, D. C. (2002) *Proc. Natl. Acad. Sci. U. S. A.* **99,** 8707–8712
9. Caron, C., Pivot-Pajot, C., van Grunsven, L. A., Col, E., Lestrat, C., Rousseaux, S., and Khochbin, S. (2003) *EMBO Rep.* **4,** 877–882
10. Kouzarides, T. (2007) *Cell* **128,** 693–705
11. Jacobs, S. A., and Khorasanizadeh, S. (2002) *Science* **295,** 2080–2083
12. Fischle, W., Wang, Y., Jacobs, S. A., Kim, Y., Allis, C. D., and Khorasanizadeh, S. (2003) *Genes Dev.* **17,** 1870–1881
13. Jacobs, S. A., Fischle, W., and Khorasanizadeh, S. (2004) *Methods Enzymol.* **376,** 131–148
14. Min, J., Zhang, Y., and Xu, R. M. (2003) *Genes Dev.* **17,** 1823–1828
15. Nielsen, P. R., Nietlispach, D., Mott, H. R., Callaghan, J., Bannister, A., Kouzarides, T., Murzin, A. G., Murzina, N. V., and Laue, E. D. (2002) *Nature* **416,** 103–107
16. Hughes, R. M., Wiggins, K. R., Khorasanizadeh, S., and Waters, M. L. (2007) *Proc. Natl. Acad. Sci. U. S. A.* **104,** 11184–11188
17. Fischle, W., Tseng, B. S., Dormann, H. L., Ueberheide, B. M., Garcia, B. A., Shabanowitz, J., Hunt, D. F., Funabiki, H., and Allis, C. D. (2005) *Nature* **438,** 1116–1122
18. Hirota, T., Lipp, J. J., Toh, B. H., and Peters, J. M. (2005) *Nature* **438,** 1176–1180
19. Fischle, W., Wang, Y., and Allis, C. D. (2003) *Nature* **425,** 475–479
20. Dormann, H. L., Tseng, B. S., Allis, C. D., Funabiki, H., and Fischle, W. (2006) *Cell Cycle* **5,** 2842–2851
21. Bernstein, E., Duncan, E. M., Masui, O., Gil, J., Heard, E., and Allis, C. D. (2006) *Mol. Cell. Biol.* **26,** 2560–2569
22. Mito, Y., Henikoff, J. G., and Henikoff, S. (2007) *Science* **315,** 1408–1411
23. Henikoff, S., and Ahmad, K. (2005) *Annu. Rev. Cell Dev. Biol.* **21,** 133–153
24. Hake, S. B., and Allis, C. D. (2006) *Proc. Natl. Acad. Sci. U. S. A.* **103,** 6428–6435
25. Govin, J., Caron, C., Rousseaux, S., and Khochbin, S. (2005) *Trends Biochem. Sci.* **30,** 357–359
26. Ong, S. E., Mittler, G., and Mann, M. (2004) *Nat. Meth.* **1,** 119–126
27. Garcia, B. A., Busby, S. A., Barber, C. M., Shabanowitz, J., Allis, C. D., and Hunt, D. F. (2004) *J. Proteome Res.* **3,** 1219–1227
28. Kuzmichev, A., Jenuwein, T., Tempst, P., and Reinberg, D. (2004) *Mol. Cell* **14,** 183–193
29. Henkels, C. H., and Khorasanizadeh, S. (2007) *Mol. Cell* **27,** 521–522
30. Sampath, S. C., Marazzi, I., Yap, K. L., Sampath, S. C., Krutchinsky, A. N., Mecklenbrauker, I., Viale, A., Rudensky, E., Zhou, M. M., Chait, B. T., and Tarakhovsky, A. (2007) *Mol. Cell* **27,** 596–608
31. Kimmins, S., and Sassone-Corsi, P. (2005) *Nature* **434,** 583–589
32. Ooi, S. L., and Henikoff, S. (2007) *Curr. Opin. Cell Biol.* **19,** 257–265
33. Bernstein, B. E., Meissner, A., and Lander, E. S. (2007) *Cell* **128,** 669–681
34. Berger, S. L. (2007) *Nature* **447,** 407–412
35. Grewal, S. I., and Jia, S. (2007) *Nat. Rev. Genet.* **8,** 35–46
36. Jacobs, S. A., Taverna, S. D., Zhang, Y., Briggs, S. D., Li, J., Eissenberg, J. C., Allis, C. D., and Khorasanizadeh, S. (2001) *EMBO J.* **20,** 5232–5241
37. Ma, J. C., and Dougherty, D. A. (1997) *Chem. Rev.* **97,** 1303–1324
38. Gallivan, J. P., and Dougherty, D. A. (1999) *Proc. Natl. Acad. Sci. U. S. A.* **96,** 9459–9464
39. Shi, Y., Sawada, J., Sui, G., Affar el, B., Whetstine, J. R., Lan, F., Ogawa, H., Luke, M. P., Nakatani, Y., and Shi, Y. (2003) *Nature* **422,** 735–738
40. Li, B., Gogol, M., Carey, M., Lee, D., Seidel, C., and Workman, J. L. (2007) *Science* **316,** 1050–1054
41. Khalil, A. M., Boyar, F. Z., and Driscoll, D. J. (2004) *Proc. Natl. Acad. Sci. U. S. A.* **101,** 16583–16587
42. Delaval, K., Govin, J., Cerqueira, F., Rousseaux, S., Khochbin, S., and Feil, R. (2007) *EMBO J.* **26,** 720–729
43. Reik, W. (2007) *Nature* **447,** 425–432
44. Flanagan, J. F., Blus, B. J., Kim, D., Clines, K. L., Rastinejad, F., and Khorasanizadeh, S. (2007) *J. Mol. Biol.* **369,** 334–342
45. Bhattacharyya, R. P., Remenyi, A., Yeh, B. J., and Lim, W. A. (2006) *Annu. Rev. Biochem.* **75,** 655–680
46. Chin, H. G., Patnaik, D., Esteve, P. O., Jacobsen, S. E., and Pradhan, S. (2006) *Biochemistry* **45,** 3272–3284
47. Fischle, W., Kiermer, V., Dequiedt, F., and Verdin, E. (2001) *Biochem. Cell Biol.* **79,** 337–348